Ratios of charged antiparticles to particles near mid-rapidity in Au+Au collisions at $\sqrt{s_{_{NN}}} = 130$ GeV

B.B.Back[1], M.D.Baker[2], D.S.Barton[2], R.R.Betts[1,6], R.Bindel[7], A.Budzanowski[3], W.Busza[4], A.Carroll[2], M.P.Decowski[4], E.Garcia[7], N.George[1], K.Gulbrandsen[4], S.Gushue[2], C.Halliwell[6], G.A.Heintzelman[2], C.Henderson[4], R.Hołyński[3], D.Hofman[6], B.Holzman[6], E.Johnson[8], J.Kane[4], J.Katzy[4,6], N. Khan[8], W.Kucewicz[6], P.Kulinich[4], W.T.Lin[5], S.Manly[8], D.McLeod[6], J.Michałowski[3], A.Mignerey[7], J.Mulmenstadt[4], R.Nouicer[6], A.Olszewski[2,3], R.Pak[2], I.C.Park[8], H.Pernegger[4], C.Reed[4], L.P.Remsberg[2], M.Reuter[6], C.Roland[4], G.Roland[4], L.Rosenberg[4], P.Sarin[4], P.Sawicki[3], W.Skulski[8], S.G.Steadman[4], G.S.F.Stephans[4], P.Steinberg[2], M.Stodulski[3], A.Sukhanov[2], J.-L.Tang[5], R.Teng[8], A.Trzupek[3], C.Vale[4], G.J.van Nieuwenhuizen[4], R.Verdier[4], B.Wadsworth[4], F.L.H.Wolfs[8], B.Wosiek[3], K.Woźniak[3], A.H.Wuosmaa[1], B.Wysłouch[4]

[1] Physics Division, Argonne National Laboratory, Argonne, IL 60439-4843

[2] Chemistry and C-A Departments, Brookhaven National Laboratory, Upton, NY 11973-5000

[3] Institute of Nuclear Physics, Kraków, Poland

[4] Laboratory for Nuclear Science, Massachusetts Institute of Technology, Cambridge, MA 02139-4307

[5] Department of Physics, National Central University, Chung-Li, Taiwan

[6] Department of Physics, University of Illinois at Chicago, Chicago, IL 60607-7059

[7] Department of Chemistry, University of Maryland, College Park, MD 20742

[8] Department of Physics and Astronomy, University of Rochester, Rochester, NY 14627

(April 10, 2001)

We have measured the ratios of antiparticles to particles for charged pions, kaons and protons near mid-rapidity in central Au+Au collisions at $\sqrt{s_{_{NN}}} = 130$ GeV. For protons, we observe $\langle\overline{p}\rangle/\langle p\rangle = 0.60 \pm 0.04(stat.) \pm 0.06(syst.)$ in the transverse momentum range $0.15 < p_T < 1.0$ GeV/c. This leads to an estimate of the baryo-chemical potential μ_B of 45 MeV, a factor of 5-6 smaller than in central Pb+Pb collisions at $\sqrt{s_{_{NN}}} = 17.2$ GeV.

PACS numbers: 25.75.-q

In this paper multiplicity ratios of antiparticles to particles for primary charged pions, kaons and protons are presented for collisions of gold nuclei at an energy of $\sqrt{s_{_{NN}}} = 130$ GeV. The data were taken with the PHOBOS detector during the first run of the Relativistic Heavy-Ion Collider (RHIC) at Brookhaven National Laboratory. The experiments at RHIC aim at understanding the behavior of strongly interacting matter at high temperature and density. Quantum chromodynamics, the fundamental theory of strong interactions, predicts that under these conditions a new state of matter will be formed, the quark-gluon plasma [1].

One of the most intriguing results from heavy-ion collisions at lower energies was the observation that particle ratios for particles with production cross-sections varying by several orders of magnitude could be described in a statistical picture of particle production assuming chemical equilibrium [2–4]. This is particularly remarkable for the production rates of rare baryons and antibaryons containing multiple strange quarks [5], which were found to be difficult to reproduce in microscopic hadronic transport models [6,7]. One of the key ingredients for the statistical particle production picture is the baryo-chemical potential μ_B. The particle ratios presented here, in particular $\langle\overline{p}\rangle/\langle p\rangle$, provide information about μ_B at RHIC energies.

On a microscopic level, the $\langle\overline{p}\rangle/\langle p\rangle$ ratio reflects the interplay between the transport of baryon number carried by protons and neutrons in the colliding nuclei in momentum space, the production of quark-antiquark pairs and the annihilation of antiprotons in the final stages of the collision. The connection between baryon number transport and the energy loss of the incoming nucleons [8] is under intense theoretical discussion [9,10].

The data reported here were collected using the PHOBOS two-arm magnetic spectrometer. Details of the setup can be found elsewhere [11–13]. One arm (SPECP) of the spectrometer was only partially equipped with 6 layers of silicon sensors, providing tracking only in the field-free region close to the beampipe. The other arm (SPECN) had a total of 16 layers of sensors, providing tracking both outside and inside the 2 T field of the PHOBOS magnet. Particles within the geometrical acceptance region used in this analysis traverse 14 or 15 of the layers. A two layer silicon detector (VTX) covering $|\eta| < 1.5$ and 25% of the azimuthal angle provided additional information on the position of the primary collision vertex. In total, 94362 sensitive detector elements were read out, of which less than 2% were non-functional.

The primary event trigger was provided by two sets of 16 scintillator paddle counters covering pseudorapidities $3 < |\eta| < 4.5$. Additional information for event selection was obtained from two zero-degree calorimeters measuring spectator neutrons. Details of the event selection and centrality determination can be found in [14,15]. Monte Carlo (MC) simulations of the apparatus were based on the HIJING event generator [16] and the GEANT 3.21 simulation package, folding in the signal response for scintillator counters and silicon sensors.

For this analysis the 12% events with the highest signal in the paddle counters were selected, corresponding to the collisions with the highest number of participating nucleons N_{part}. The average number of participants for the selected events was estimated as $\langle N_{part} \rangle = 312 \pm 10$(syst.), using a Glauber calculation relating N_{part} to the fractional cross section observed in bins of the paddle signal [14,15].

As the geometrical layout of the PHOBOS detector leads to an asymmetry in the acceptance and detection efficiency for positive and negatively charged particles for a given magnet polarity, data was taken using both magnet polarities (BPLUS and BMINUS). The reproducibility of the absolute field strength was found to be better than 1%, based on Hall probe measurements for each polarity and the comparison of mass distributions for identified particles for the two polarities.

The stability of the trigger event selection was checked using the number of reconstructed straight line particle tracks outside the magnetic field. The straight track multiplicities for the BPLUS and BMINUS data sets agreed to within 0.2%.

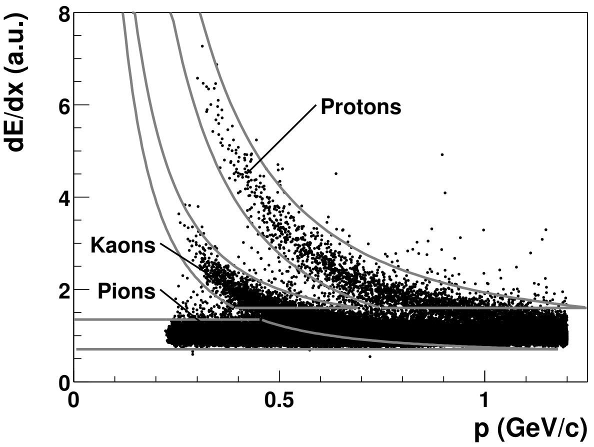

FIG. 1. Distribution of average energy loss as a function of reconstructed particle momentum. Three clear bands can be seen, corresponding to pions, kaons and protons. The solid lines indicate the cut regions for counting identified particles.

To optimize the precision of the vertex and track finding only events with a reconstructed primary vertex position between -16 cm $< z_{vtx} <$ 10 cm along the beam axis were selected. We also restricted the analysis to tracks in the central region of the spectrometer planes along the 45° axis of the experiment. A precise knowledge of the primary vertex for each event is essential for this analysis, as the distance of closest approach of each reconstructed track with respect to the primary vertex (dca_{vtx}) is the only tool for rejecting background particles from decays and secondary interactions. By requiring a consistent vertex position from the SPEC and VTX subdetectors, in combination with the known position of the beam orbit, a vertex resolution better than 0.3 mm (RMS) in y and z directions and better than 0.5 mm in x direction was achieved.

Particle tracks in the spectrometer were reconstructed as follows: tracks in the first 6 layers outside the magnetic field were reconstructed by a road-following algorithm.

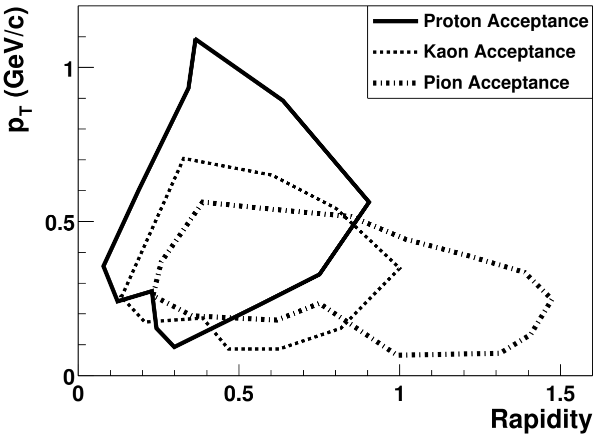

FIG. 2. Acceptance of the spectrometer as a function of transverse momentum and rapidity for pions, kaons and protons. The acceptance is averaged over the accepted vertex range and azimuthal angle ϕ.

Inside the field, two-hit combinations on consecutive layers were mapped into $(1/p, \Theta)$ space, where Θ is the polar angle at the primary interaction vertex and p the total momentum. A clustering algorithm then selected combinations of matching hits in $(1/p, \Theta)$ space, yielding track pieces inside the field. For track pieces inside and outside the field, the specific ionization dE/dx was calculated using the truncated mean of the angle-corrected hit energies, discarding the 30% highest energy values. Straight and curved track pieces where then matched based on Θ, a fit to the combined track in the yz-plane and requiring consistency in the independently determined dE/dx values.

For the matched tracks the dE/dx was again calculated using a 30% truncation. Particle identification was performed using p and dE/dx, which depends only on particle velocity. The identification cuts are shown in Fig. 1 with three bands corresponding to pions, kaons and protons. The corresponding acceptance regions for identified particles in transverse momentum p_T and rapidity are shown in Fig. 2. Table I gives the resulting event and identified particle statistics for all combinations of magnet polarity, particle charge and particle mass, as well as the uncorrected average transverse momentum $\langle p_T \rangle$. Using two magnetic field settings allows the determination of two statistically independent values for each of the three particle ratios. As can be seen from Table I, the two values agree within statistical uncertainty for each of the ratios.

Preliminary PHOBOS data show a total multiplicity of produced charged particles $N_{ch} \approx 3500$ [17] for the event selection used here. This is large compared to the average initial charge asymmetry given by the number of participating protons of $\langle N^p_{part} \rangle \approx 125$. The charge asymmetry $1-\langle N^-\rangle/\langle N^+\rangle$ in the final state will therefore be small, so that a random contamination of the identified particle samples would move the observed ratios towards unity. The contamination of the proton and antiproton samples was checked by testing the stability of the antiproton/proton ratio against variation of the particle-ID cuts shown in Fig. 1. Within statistical error the ratios were stable against further changes of the cuts.

For comparison with data from other experiments and theoretical calculations several corrections to the observed particle ratios have to be applied. These corrections account for particles produced in secondary interactions, loss of particles due to absorption in detector material, and feeddown particles from weak decays. Both feeddown and secondary particles tend to be produced with lower p_T than the corresponding primary particles. Simulations show that the difference in contamination of π^+ and π^- by positrons and electrons, which cannot be rejected within the resolution of the dE/dx measurement, is negligible.

The acceptance for secondary and feeddown particles is limited to those produced within 10 cm radial distance to the primary collision vertex, as accepted tracks were required to have at least one hit in the first two layers of the spectrometer. The background contamination is further reduced by requiring the particle tracks to have $dca_{vtx} < 3.5$ mm.

As HIJING reproduces the total charged particle multiplicity near mid-rapidity to within 10%, the simulation should give an accurate estimate of the background from secondary interactions. The correction factors are shown in Fig. 3 as a function of transverse momentum. The net correction is 0.01 for $\langle\overline{p}\rangle/\langle p\rangle$. For pions and kaons the contribution from secondary particles is much less than 1%. The difference in absorption for protons and antiprotons in the detector material was studied based on GEANT simulations. The fraction of absorbed protons and antiprotons as a function of p_T is also shown in Fig. 3. From this correction, which averages to 1.7% for the protons and 6.3% for the antiprotons a correction to $\langle\overline{p}\rangle/\langle p\rangle$ of 0.04 is obtained. The contribution from feeddown particles can not be modelled as precisely, as the absolute yield of strange hadrons has not yet been measured at RHIC.

TABLE I. Number of accepted events, uncorrected number of identified particles and uncorrected $\langle p_T\rangle$ for each magnetic field polarity.

	BPLUS 26509 events		BMINUS 41580 events	
	# of particles	$\langle p_T\rangle$ (MeV/c)	# of particles	$\langle p_T\rangle$ (MeV/c)
π^+	6208	412 ± 1	23223	254 ± 1
π^-	14783	253 ± 1	9679	410 ± 1
K^+	136	358 ± 4	256	248 ± 4
K^-	146	255 ± 5	198	366 ± 4
p	223	581 ± 10	331	475 ± 8
$\overline{p}$	109	481 ± 12	218	560 ± 8

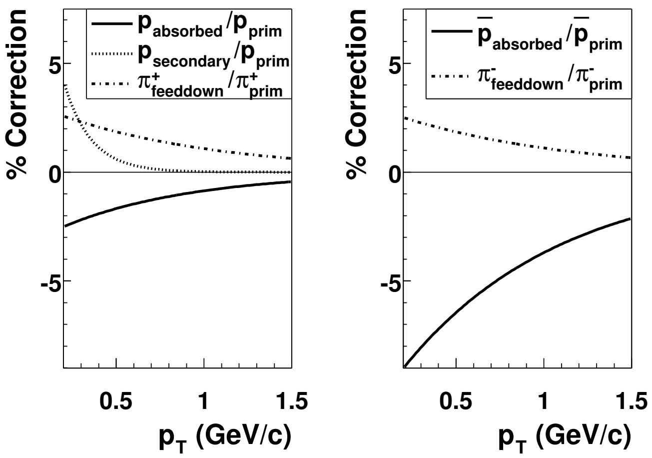

FIG. 3. Correction factors for particle multiplicities as a function of transverse momentum p_T for positive and negative particles. Correction factors of less than 1% and the p_T-independent feeddown correction for $\langle\overline{p}\rangle/\langle p\rangle$ are not shown.

Simulations show that the feeddown correction for $\langle K^-\rangle/\langle K^+\rangle$ and $\langle\pi^-\rangle/\langle\pi^-\rangle$ (see Fig. 3) is less than 1%, whereas feeddown to protons and antiprotons from Λ and $\overline{\Lambda}$ is not negligible. The feeddown correction to the $\langle\overline{p}\rangle/\langle p\rangle$ ratio can be evaluated as a function of the $\langle\overline{\Lambda}\rangle/\langle\Lambda\rangle$ and $\langle\Lambda\rangle/\langle p\rangle$ ratios. Transport model studies, as well as quark counting arguments and data from lower energies show that to a good approximation the following relationship holds [18]:

$$\frac{\langle\overline{\Lambda}\rangle}{\langle\Lambda\rangle} = \frac{\langle K^+\rangle}{\langle K^-\rangle}\cdot\frac{\langle\overline{p}\rangle}{\langle p\rangle}$$

Our data show $\langle K^+\rangle/\langle K^-\rangle = 1.1$, suggesting only a 10% difference in $\langle\overline{\Lambda}\rangle/\langle\Lambda\rangle$ compared to $\langle\overline{p}\rangle/\langle p\rangle$. Using the $dca_{vtx} < 3.5$ mm cut, less than half of the protons from weak decays are accepted in the analysis. This further reduces the feeddown correction to $\langle\overline{p}\rangle/\langle p\rangle$. Using MC simulations, the range of the correction was estimated by varying the $\langle\Lambda\rangle/\langle p\rangle$ ratio from 0.2, the value predicted by HIJING, to 0.4 and varying $\langle K^+\rangle/\langle K^-\rangle$ from 1 to 1.2. The resulting correction to $\langle\overline{p}\rangle/\langle p\rangle$ ranges from 0 to -0.03, with a most probable value of -0.01.

After corrections we find the following ratios within our acceptance:

$$\langle\pi^-\rangle/\langle\pi^+\rangle = 1.00 \pm 0.01(\text{stat.}) \pm 0.02(\text{syst.})$$
$$\langle K^-\rangle/\langle K^+\rangle = 0.91 \pm 0.07(\text{stat.}) \pm 0.06(\text{syst.})$$
$$\langle\overline{p}\rangle/\langle p\rangle = 0.60 \pm 0.04(\text{stat.}) \pm 0.06(\text{syst.})$$

For all three particle species the average transverse momentum of antiparticles and particles agrees within statistical error (see Table I), indicating no strong dependence of the ratios on transverse momentum.

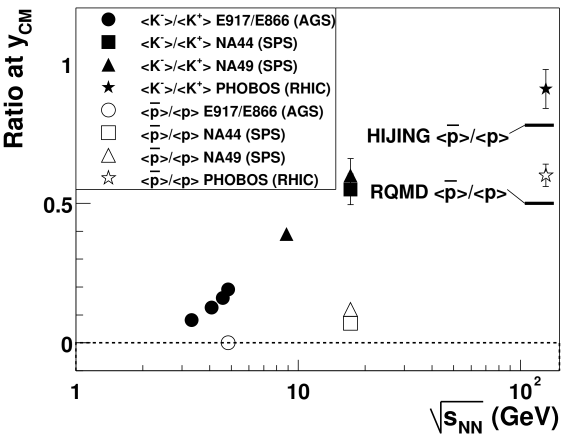

FIG. 4. $\langle K^- \rangle / \langle K^+ \rangle$ and $\langle \overline{p} \rangle / \langle p \rangle$ ratios as a function of $\sqrt{s}$ for nucleus-nucleus collisions, in comparison with predictions from the HIJING and RQMD models. Only statistical errors are shown.

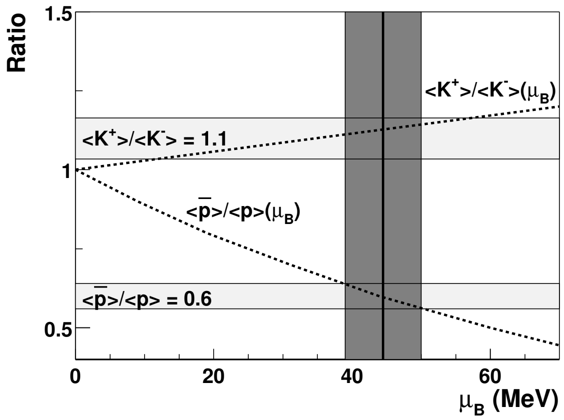

FIG. 5. Statistical model calculation (dotted lines) of $\langle K^- \rangle / \langle K^+ \rangle$ and $\langle \overline{p} \rangle / \langle p \rangle$ as a function of μ_B by Redlich et al. The horizontal bands show the ratios observed in the data (statistical errors only). The vertical shaded area indicates the allowed region in μ_B.

In Fig. 4 our results are compared to lower energy data [19–21] and calculations using the HIJING and RQMD [7] microscopic transport models. The values for the $\langle K^- \rangle / \langle K^+ \rangle$ and $\langle \overline{p} \rangle / \langle p \rangle$ ratios are significantly higher than at lower energies. Using the same parameters that successfully described the charged particle multiplicity density in Au+Au collisions at RHIC [14], HIJING overestimates $\langle \overline{p} \rangle / \langle p \rangle$ by 0.18. Clearly, the particle ratio data provide additional constraints for microscopic models. A better description may require a modification in the baryon number stopping mechanism, baryon-pair production or antibaryon annihilation. An indication of possible mechanisms is given by the comparison with RQMD, which includes rescattering of produced hadrons and predicts a value for $\langle \overline{p} \rangle / \langle p \rangle$ that is 0.1 below our data.

Finally, we estimate the baryo-chemical potential μ_B using a statistical model calculation [22] shown in Fig. 5. For a realistic range of freeze-out temperatures of 160 to 170 MeV, both $\langle K^+ \rangle / \langle K^- \rangle$ and $\langle \overline{p} \rangle / \langle p \rangle$ are consistent with $\mu_B = 45 \pm 5$ MeV. This is much lower than the value of $\mu_B = 240 - 270$ MeV [**?**,4] obtained in thermal fits to Pb+Pb data at $\sqrt{s_{NN}} = 17.2$ GeV, showing a closer but not yet complete approach to a baryon-free regime at RHIC.

This work was partially supported by US DoE grants DE-AC02-98CH10886, DE-FG02-93ER-404802, DE-FC02-94ER40818, DE-FG02-94ER40865, DE-FG02-99ER41099, W-31-109-ENG-38. NSF grants 9603486, 9722606 and 0072204. The Polish groups were partially supported by KBN grant 2 P03B 04916. The NCU group was partially supported by NSC of Taiwan under contract NSC 89-2112-M-008-024.

[1] See e. g. J. P. Blaizot, Nucl. Phys. **A661** (1999) 3.
[2] E. Schnedermann, J. Sollfrank, U. Heinz, Phys. Rev. **C48** (1993) 2462.
[3] F. Becattini, Z. Phys. **C69** (1996) 485.
[4] P. Braun-Munzinger, I. Heppe, J. Stachel, Phys. Lett. **B465** (1999) 15.
[5] P. Koch, B. Müller, J. Rafelski, Phys. Rep. **C142** (1986) 167.
[6] S. A. Bass et al., Prog. Part. Nucl. Phys. **41** (1998) 225.
[7] H. Sorge, Phys. Rev. **C52** (1995) 3291.
[8] W. Busza, A. S. Goldhaber, Phys. Lett. **B139** (1984) 235.
[9] D. Kharzeev, Phys. Lett. **B378** (1996) 238.
[10] S. E. Vance, M. Gyulassy, X. N. Wang, Phys. Lett. **B443** (1998) 45.
[11] B. Back et al., Nucl. Phys. **A661** (1999) 690.
[12] H. Pernegger et al., Nucl. Instrum. Methods. **A419** (1998) 549.
[13] R. Pak, PHOBOS Collaboration, proceedings of Quark Matter '01 Conference (in press).
[14] B. Back et al., Phys. Rev. Lett. **85** (2000) 3100.
[15] J. Katzy et al., PHOBOS Collaboration, proceedings of Quark Matter '01 Conference (in press).
[16] M. Gyulassy and X. N. Wang, Comp. Phys. Comm. 83 (1994) 307. We used HIJING V1.35 with standard parameter settings.
[17] A. Wuosmaa et al., PHOBOS Collaboration, proceedings of Quark Matter '01 Conference (in press).
[18] J. Zimanyi, Nucl. Phys. **A661** (1999) 224.
[19] L. Ahle et al., Phys. Lett. **B490** (2000) 53,
Phys. Rev. **C60**, (1999) 064901,
Phys. Rev. Lett. **81**, (1998) 2650 .
[20] J. Bächler et al., Nucl. Phys. **A661** (1999) 45.
[21] I. G. Bearden et al., Phys. Lett. **B388** (1996) 431.
[22] K. Redlich, proceedings of Quark Matter '01 Conference (in press).